Intermetallics 77 (2016) 34–40

Contents lists available at ScienceDirect

Intermetallics

journal homepage: www.elsevier.com/locate/intermet

Ductile to brittle transition of fracture of a Zr-based bulk metallic glass: Strain rate effect

M.C. Li [a], M.Q. Jiang [b], G. Li [a], L. He [a], J. Sun [a], F. Jiang [a, *]

[a] State Key Laboratory for Mechanical Behavior of Materials, Xi'an Jiaotong University, Xi'an 710049, China
[b] State Key Laboratory of Nonlinear Mechanics, Institute of Mechanics, Chinese Academy of Sciences, Beijing 100190, China

ARTICLE INFO

Article history:
Received 20 May 2016
Received in revised form
16 June 2016
Accepted 11 July 2016
Available online 25 July 2016

Keywords:
Metallic glasses
Fracture
Strain rate
Ductile-to-brittle transition

ABSTRACT

Quasi-static and dynamic tensile experiments were conducted on a Zr-based bulk metallic glass at room temperature. A significant ductile-to-brittle transition was identified with increasing strain rate, based on the changes in the macroscopic fracture mode from shear to normal tension and in the microscopic fracture feature from vein patterns to fine dimples and/or nanoscale periodic corrugations. According to the Mohr-Coulomb criterion, it is revealed that such a transition is due to the competition between the intrinsic critical shear and tensile strengths at different strain rates. Microscopically, the strain-rate-induced transition is attributed to the change in the motion of local atomic groups from shear transformation zone to tension transformation zone, in which the characteristic volume of shear transformation zone is a key parameter.

© 2016 Published by Elsevier Ltd.

1. Introduction

The physics of ductile-to-brittle transition (DBT) has been one of the long-standing issues in the materials field [1,2]. When subjected to a stress, many crystals, such as body-centered cubic metals and silicon, exhibit brittle fracture below a critical temperature whereas a plastic flow above this temperature, which is defined as the DBT temperature and mainly determined by the dislocation movements [1]. Due to the lack of long-range order, metallic glasses are free of dislocations, grain boundaries, crystallographic planes, etc. It is therefore expected that the DBT behavior would not occur in metallic glasses. However, Wu and Spaepen [3] found an apparent DBT behavior in a Fe-based metallic glass ribbon as the temperature decreased across a critical value. From then on, the DBT phenomena have been widely observed in various metallic glasses [4–12], and attracted much attention due to its scientific and practical significance. The advances regarding this aspect have been reviewed recently [13,14]. It has been widely accepted that the DBT of metallic glasses is indicated by the changes in the macroscopic fracture mode from shear to normal tension and in the microscopic fracture morphology from vein patterns to fine dimples and/or nanoscale periodic corrugations [12,15–21]. In the meantime, there are also many literatures [22–27] demonstrated the absence of DBT behavior in metallic glasses under compression with decreasing temperature. This may due in large part to: (i) the DBT behavior is hard to occur under uniaxial compression as the tensile stress will gradually increase from zero, deriving from the shear induced dilatation during compressive loading. As a consequence, the samples should first shear, and then continue to fail in shear fracture mode or tensile fracture mode [19,21]. (ii) the reported enhanced compressive plasticity under cryogenic temperature might originate from the single shear band sliding along the principle shear plane as the velocity of shear-banding equals to that applied on the test machine cross-head [28,29], in addition, the geometrical constraints will also play an important role on the enhancement of the compressive plasticity [30].

According to the cooperative shear model, the volume of shear transformation zone (STZ) has been proposed to be an effective indicator of the DBT of metallic glasses [31], which is theoretically modeled by Jiang et al. [18]. The model predicts that decreasing temperature, reducing free volume and/or increasing strain rates can decrease the STZ volume; hence, it needs a large number of STZs to activate a flow event, which might be hard to synchronously cooperate shearing. As a result, the brittle fracture associated with tension transformation zones (TTZs) induced nano-cavitation will take place [32], instead of the ductile fracture dominated by STZ-mediated shear banding [33]. The former two factors (temperature and free volume) have been confirmed by experiments

* Corresponding author.
E-mail address: jiangfeng@mail.xjtu.edu.cn (F. Jiang).

http://dx.doi.org/10.1016/j.intermet.2016.07.004
0966-9795/© 2016 Published by Elsevier Ltd.

[18–21], while the third one (strain rate) has been rarely shed light on [34]. The present work is dedicated to investigate the effect of strain rate on the properties of a typical Zr-based bulk metallic glass with different free volume levels. The macroscopic mechanical responses and microscopic fracture morphologies demonstrated an obvious DBT behavior, which is induced by the increasing of the applied strain rate. The underlying mechanism is discussed as well.

2. Experiments

A typical $Zr_{52.5}Cu_{17.9}Ni_{14.6}Al_{10}Ti_5$ (Vit105) bulk metallic glass was chosen as the model material. The plates with dimensions of $40 \times 20 \times 2$ mm^{3}were prepared using the drop casting method, and then machined into the Dog-bone-shaped samples with gauge dimensions of $6 \times 1 \times 0.8$ mm^3 for the tensile tests. Some samples were sealed in evacuated quartz capsules and annealed below the glass transition temperature (T_g = 690 K). Thus, there were four groups of samples labeled as "a", "b", "c" and "d", respectively. Sample "a" was as-cast. Samples "b", "c" and "d" were annealed at 575 K, 600 K and 650 K for 30 min, respectively. The surfaces of all specimens were polished to remove oxides. The glassy state of all samples was verified by X-ray diffraction and high resolution transmission electron microscopy. The free volume changes were indirectly measured using the differential scanning calorimetry (DSC) method. The DSC tests were conducted using a TA Q2000 thermal-analysis instrument with a heating rate of 0.33 K/s in a flow of argon, and a second run under identical conditions was used to determine the base line after each measurement. It should be noted that, for the BMGs, three-point bending is a more effective method to study the variation of plastic deformation ability than uniaxial compression and tension. In other words, it is a better way to characterize the DBT behavior of BMGs. However, it is relatively more difficult to perform super high strain rate tests under three-point bending than uniaxial tension. Therefore, uniaxial tension tests were used to reveal the strain rate effect on the DBT behavior of the metallic glass in this study. Quasi-static tensile experiments were performed in a computer-controlled SUNS CMT 5105 material testing machine at a nominal strain rate of 2.0×10^{-4} s^{-1} and the dynamic ones were carried out using Split Hopkinson Tensile Bar (SHTB) at a strain rate of about 1.8×10^3 s^{-1}. At least 6 samples were tested at each case to ensure the reliability of the experimental results. After tests, the fracture angles and the morphologies of fracture surfaces of the samples were examined by a scanning electron microscopy (SEM; SU6600).

3. Results

The DSC curves of all the samples used in this study are shown in Fig. 1. Obviously, they exhibit very similar thermal behaviors with a distinct glass transition before crystallization. However, the amplification of the exothermic signals before the glass transition exhibits an apparent difference among these samples, which is presented in the inset of Fig. 1. It is well known that the exothermic event ΔH (i.e. the heat release during relaxation) prior to T_g could be an indicator of the excess free volume v_f in metallic glasses with an empirical equation of $\Delta H = \beta' v_f$[35,36], where β' is a constant of the material. According to the measured ΔH and the reference state in the previous work [18], it is easy to obtain the relative free volume concentration $v_f/\Delta v^*$ normalized by a critical volumeΔv^* for the present samples, where Δv^* is required excess free volume to transition and should be at least larger than an atom volume. The $v_f/\Delta v^*$ is estimated to be 1/10, 1/14, 1/16, and 1/27 in an order: samples "a", "b", "c" and "d".

The engineering tensile stress–strain curves of the four groups of samples "a", "b", "c" and "d" under both strain rates are displayed in Fig. 2 (the curves for the dynamic tests have been smoothed). As expected that all samples exhibit the linear elastic deformation and immediate fracture without any macroscopic plastic strain. Here, it must be addressed that the bending of the curves in the dynamic cases does not mean any plasticity, but is due to the inevitably unstable signal of the measured strain. It is noted that increasing

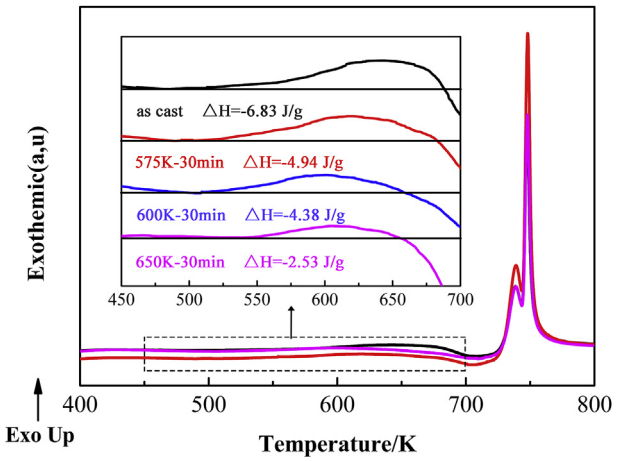

Fig. 1. DSC curves of the as-cast and annealed Vit105 samples. The inset shows the different exothermic signals before the glass transition among these samples.

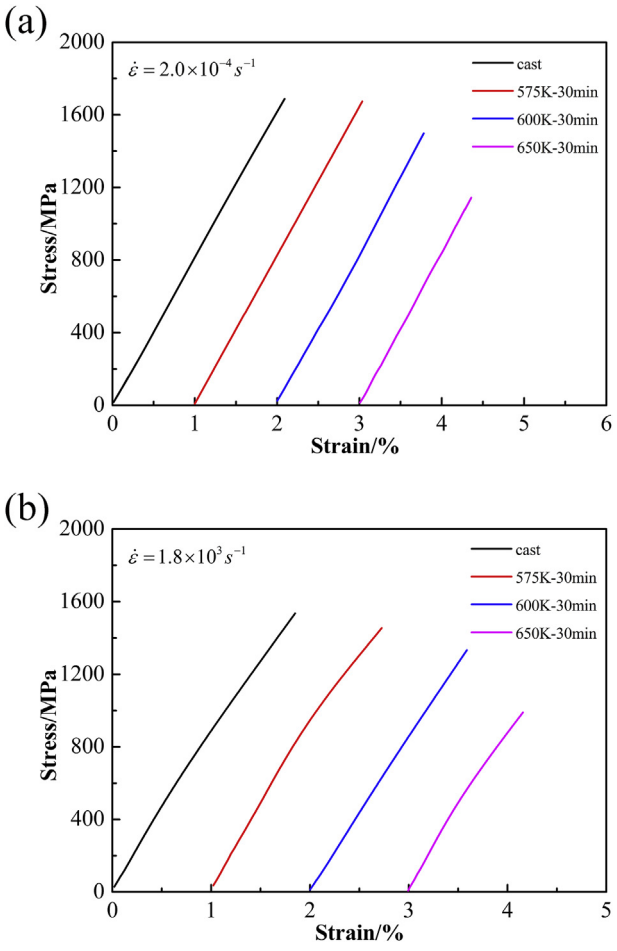

Fig. 2. The engineering stress-strain cures of the samples under: (a) quasi-static tensions and (b) dynamic tensions.

strain rate by 7 orders of magnitude does not lead to a significant increase of fracture strength σ_F but a slight decrease. In addition, under either the quasi-static or dynamic case, the fracture strength shows an apparent decrease with the reduction of the excess free volume.

Macroscopic fracture modes of these samples are presented in Fig. 3. Under the quasi-static cases, the fracture angles θ of the samples "a", "b", "c" and "d" increase gradually from 55°, 56°, 58° to 63° with decreasing excess free volume (Fig. 3(a), (c), (e) and (g)). These angles fall in the common range for metallic glasses in uniaxial tensions [20,37–39]. This implies that the fracture in these cases is shear-dominated, but the normal stress effect is improved. In contrast, the dynamic fracture angles show an obvious change from shear to tension due to the free volume decrease. The samples "a" and "b" display the typical shear fracture angles (Fig. 3(b) and (d)). For the sample "c", the fracture angle is about 71° (Fig. 3(f)), showing a remarkable departure from the maximum shear stress direction (45°). This means that the fracture of the sample "c" under the dynamic case may be not controlled by shear; instead the tension stress could play a significant role. For the sample "d", the fracture plane is approximately perpendicular to the tensile axis, with a fracture angle of about 87° (Fig. 3(h)). This clearly indicates that the fracture of the sample "d" is dominated by mode I or tension cracking rather than shear banding.

Fig. 4 shows the microscopic fracture surface morphologies of these samples. Under the quasi-static tensions, the samples "a", "b", "c" and "d" display the fracture surface morphologies similar to each other, which mainly consist of microscopic smooth cores and vein patterns (Fig. 4(a), (c), (e) and (g)). It has been widely accepted that the smooth cores correspond to local nucleation sites of the cracks owing to the existence of the normal tensile stress on the fracture planes [40–42]. The vein-partners which have been illuminated well by Saffman-Taylor flow instability of the crack front [43] strongly suggests that the failures of these samples are controlled by shear stress and the fracture is a typical ductile fracture mode. Under the dynamic cases, the samples "a" and "b" remain the ductile shear-fracture mode with the typical core-vein patterns, but with many molten droplets distributed randomly on the fracture surfaces (Fig. 4(b) and (d)). It is believed that the molten droplets are caused by the instantaneous release of the stored elastic energy during fracture [14,44]. For the sample "c", the fracture surface presents fine dimples and voids as shown in Fig. 4(f). The advent of the fine dimples and voids indicates a brittle fracture that is dominated by the cavitation ahead of the crack tip [20,45], which is consistent with the large fracture angle of about 71° (Fig. 3(f)). Nanoscale periodic corrugations with the nature of cavitation become the dominate morphologies on the fracture surface of the sample "d" (Fig. 4(h)), which agrees well with the macroscopic tension-fracture mode (Fig. 3(h)). It is worth noting that the increase of the applied strain rate can change the fracture mode of the samples "c" and "d" from shear- to tension-dominated and the fracture surface morphologies from microscopic vein-patterns to fine dimples or nanoscale periodic corrugations, respectively. This provides solid evidence that increasing strain rate can incur a DBT behavior of metallic glasses, although it is difficult for the samples with a relatively high free volume (for example, the samples "a" and "b").

Furthermore, the observed average sizes w of local nucleation sites of the cracks was used to estimate the fracture toughness K_C with the Dugdale approximation [6,12,46]:

$$K_C = \sigma_Y (6\pi w)^{1/2} \quad (1)$$

where σ_Y is the yield stress, here close to fracture strength. Based on Figs. 2 and 4, it is easy to find that the estimated K_C under the quasi-static cases is in the range from 22.2 MPa$\sqrt{\text{m}}$ of sample "a" to 13.7 MPa$\sqrt{\text{m}}$ of sample "d", which is close to the fracture toughness of the typical ductile Zr-based metallic glasses [47]. With increasing strain rate to the dynamic level, the K_C of samples "a" and "b" is nearly the same as those of the quasi-static one. However, the K_C of samples "c" and "d" decreases to 5.2 MPa$\sqrt{\text{m}}$ and 1.2 MPa$\sqrt{\text{m}}$,respectively, which is close to the typical toughness values of very brittle silicon glasses or Mg-based metallic glasses [48]. This result further confirms that the increase of stain rate can induce a DBT in metallic glasses, especially for these heavily annealed samples (for example, the samples "c" and "d").

Combining the experimental observations with the estimated fracture toughness, it is obviously found that the increase of strain rate and/or the decrease of excess free volume can lead to a DBT behavior of metallic glasses. The free volume effect on the DBT behavior of metallic glasses was investigated previously [18,19,21]. Here, a careful analysis will be made only on the effect of applied strain rate.

4. Discussion

The present experiments clearly demonstrate that, under the uniaxial tensile loading, a metallic glass can show two typical

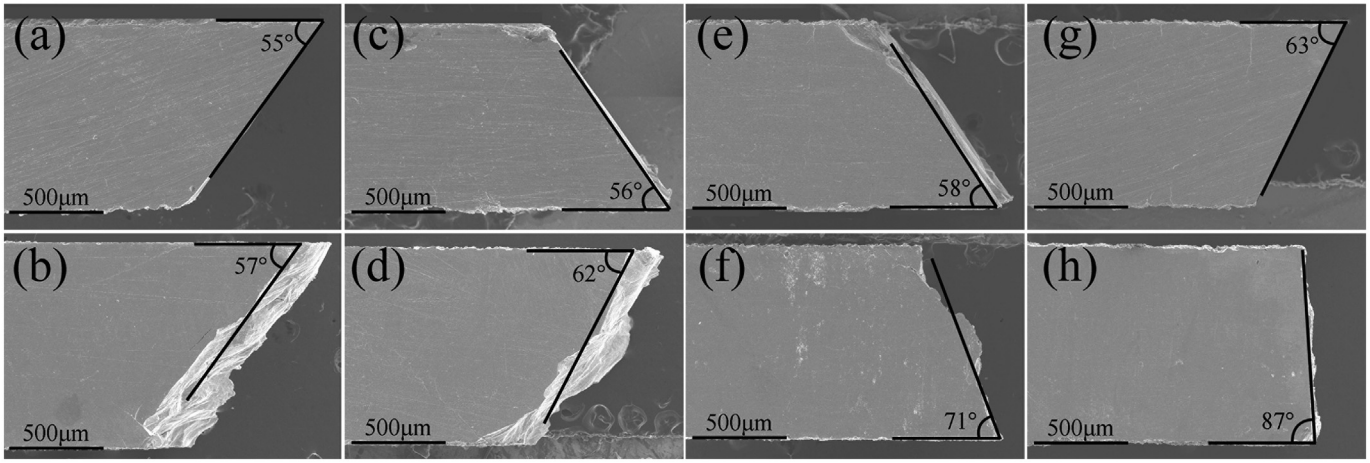

Fig. 3. Macroscopic fracture modes of samples "a", "b", "c" and "d": (a, c, e, g) the quasi-static tensions and (b, d, f, h) the dynamic tensions.

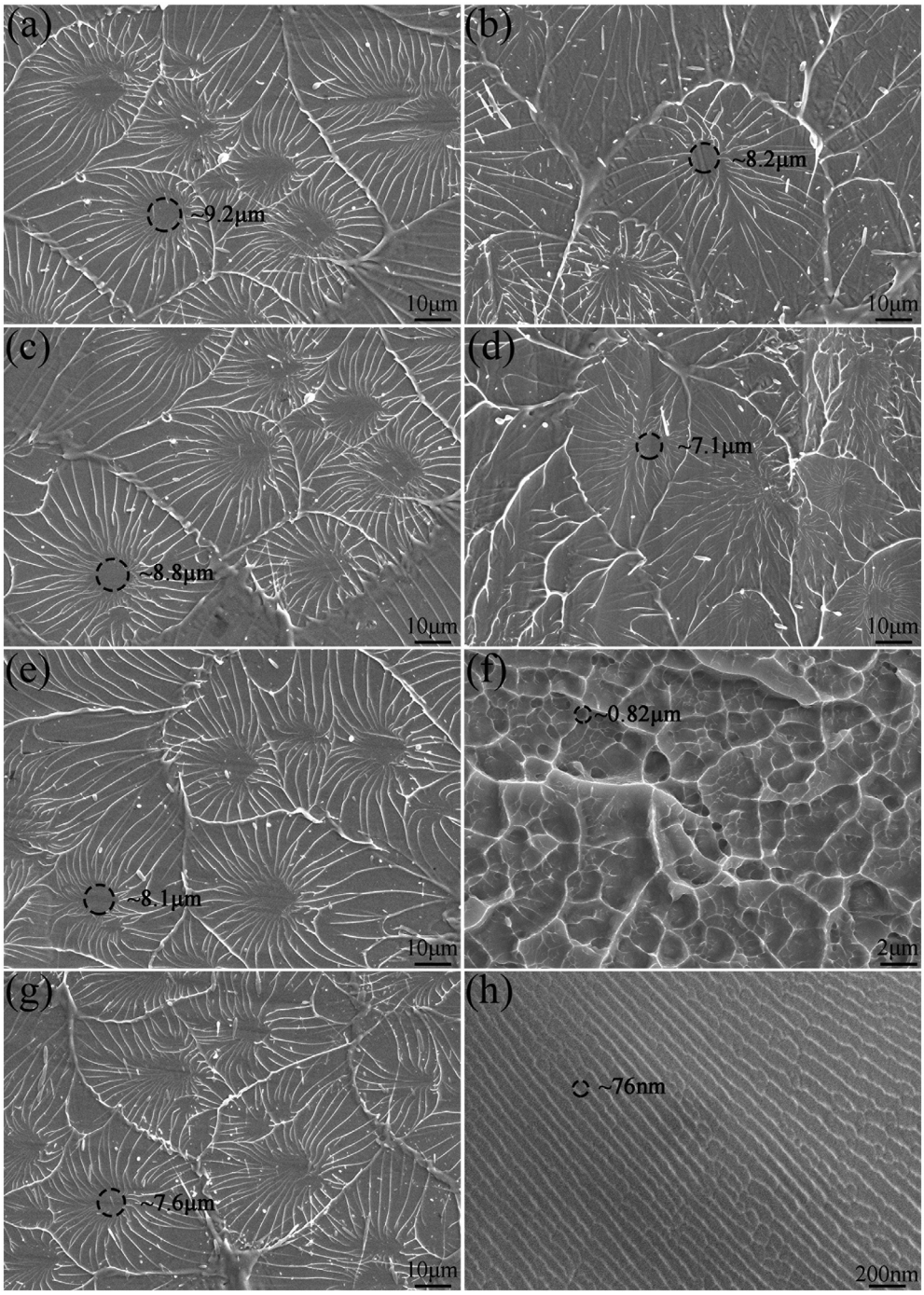

Fig. 4. Microscopic fracture morphologies of samples "a", "b", "c" and "d": (a, c, e, g) the quasi-static tensions and (b, d, f, h) the dynamic tensions.

fracture modes, i.e., shear- and tension-dominated. Which one will take place depends on the relative magnitude of τ_0 and σ_0 [20,49], which are the critical fracture stresses in pure shear and in normal tension, respectively. If τ_0 is smaller than σ_0, the shear fracture will be preferentially achieved, otherwise the fracture occurs in the normal tension mode. Based on the above observations, both τ_0 and σ_0 are free volume and strain rate dependent. The inherent competition between shear and tension in determining the fracture of metallic glasses can be well described by the Mohr-Coulomb criterion [50–52], which is expressed as:

$$\tau_0 = \tau_\theta + \alpha\sigma_\theta \tag{2}$$

where τ_θ and σ_θ are the shear and normal stresses on the fracture plane, respectively, and can be derived from:

$$\tau_\theta = \sigma_F \sin(\theta)\cos(\theta) \tag{3}$$

$$\sigma_\theta = \sigma_F \sin^2(\theta) \tag{4}$$

under the uniaxial tension condition, the normal stress sensitivity coefficient$\alpha = \tau_0/\sigma_0$ is directly related to the fracture angle θ:

$$\alpha = -\frac{\cos(2\theta)}{\sin(2\theta)} \tag{5}$$

In light of the measured fracture strength σ_F (Fig. 2) and fracture angleθ (Fig. 3), it is easy to calculate α, τ_0, and σ_0 of all the samples under the two strain rates. Fig. 5 presents the variation of τ_0 and σ_0, where the dashed lines are just guide for the eye. It can be seen that, under the quasi-static tensions, the values of τ_0 are always below these of σ_0 for all samples. This implies that the shear-induced fracture will preferentially occur. Furthermore, the difference between τ_0 and σ_0 decreases with decreasing free volume, demonstrating the enhancement of the normal stress effect. This agrees well with the observation that the fracture angles deviate from the maximum shear stress direction (45°) more significantly at the lower free volume (Fig. 3). However, the dynamic tensions display a very different trend. As for the samples "a" and "b" with the relatively high free volume, their τ_0 values are smaller than the corresponding σ_0 values, confirming the shear fracture. However, to the samples "c" and "d" with the relatively low free volume, their τ_0 values become larger than the corresponding σ_0 values, denoting the occurrence of the normal tension fracture. In fact, only when $\tau_0 > \sqrt{2}\sigma_0/2$ [37,38], the tension fracture takes place. Obviously, the increase of strain rates reduces the critical normal stress, on the other hand, increases the critical shear stress. Such a trend becomes much more remarkable as the excess free volume decreases. Below a critical free volume, the increased critical shear stress will exceed the reduced critical normal stress or precisely $\tau_0 > \sqrt{2}\sigma_0/2$. Thus, the tension fracture dominates the failure of metallic glasses. The above analysis further confirms that increasing strain rate can change the relative competition between critical shear and tension stresses of fracture, inducing the DBT of metallic glasses with relatively low free volume.

Microscopically, the observed DBT of metallic glasses induced by high strain rates can be understood as the transition of atomic-cluster motions at the crack tip from STZ-type to TTZ-type. During such a transition, the characteristic volume of STZ is a key parameter that depends on the applied strain rates. The STZ, as the fundamental deformation unit of metallic glasses, describes a collective motion around a high free volume site to accommodate the local shear strain [32–35]. The cooperative shear model developed by Johnson and Samwer [53,54]relates the onset of plastic flow of metallic glasses to the activation of STZs in the framework of potential energy landscape. By considering free-volume-assisted STZs, Jiang et al. [18] previously derived the characteristic volume of an STZ in a metallic glass with the excess free volume v_f sheared at the ambient temperature T under the strain rate $\dot{\gamma}$:

$$\Omega = \Phi(T)\left(\ln\frac{\omega_0}{C\dot{\gamma}} - \frac{\Delta v^*}{v_f}\right) \tag{6}$$

where $\Phi(T) = \frac{k_B T}{4R\zeta\mu_T\gamma_T^2(1-2\mu_T\gamma_T/(\pi\mu_0\gamma_0))^{\frac{3}{2}}}$.$\Omega$ is the actual STZ volume. ω_0 is the frequency of shear phonon of nm wavelength (~10^{13} Hz) and C is a dimensionless constant of order unity. Constant R is the "fold ratio" ≈1/4 and $\zeta = 3$ is a correction factor. k_B is the Boltzmann's constant and $\gamma_0 = 0.036$ is the critical yielding strain. μ_T is the temperature-dependent shear modulus, expressed by $\mu_T = \mu_0 - d\mu_{0T}/dT \times T$ (GPa/K) with the athermal shear modulus μ_0. The yield elastic limit has the form $\gamma_T = 0.036 - 0.016(T/T_g)^{2/3}$.The detailed definitions or values of ω_0, Δv^*, R, ζ, μ_T, γ_T, μ_0, γ_0, C, k_B, can be found in Refs. [18,53].

Eq. (6) indicates that the STZ volume decreases with increasing applied strain rate. This prediction can be rationalized by considering two extreme conditions at a fixed temperature: (i) the strain rate is high enough, and thus the STZ volume will be extremely small or close to zero because the time is too short to activate the STZs; instead, the dilatation-dominated motions of atomic cluster, i.e., TTZs, will take place; (ii) the strain rate is very slow, in which case the rearrangements of atoms and associated free volume will be sufficient to activate the STZs, finally contributing to the plastic flow. As a consequence, it is reasonable to conclude that there is a critical value of the applied strain rate corresponding to the critical volume of STZ, $\Omega_{critical}$, which could be 0.17 nm^3 or smaller [18], at a fixed temperature.

Based on Eq. (6), it is easy to calculated the STZ volume as a function of the strain rates from 10^{-5} to 10^5 s^{-1} for the different free volume values $v_f/\Delta v^*$ corresponding to the samples "a", "b", "c" and "d", as shown in Fig. 6. It is apparent that the STZ volume will decrease monotonously with the increase of the applied strain rate. For the samples "a" and "b", the calculated values of STZ volume are positive and larger than the critical one under the two strain rates adopted in this study (the points circled by dashed ellipses in Fig. 6). This means the STZs can be activated and the final fracture will be dominated by STZ-mediated shear banding, resulting in the mode II fracture (Fig. 3). As to the samples "c" and "d" under the quasi-static tensions, their STZ volumes are also larger than the critical value, denoting a shear fracture. With increasing strain rate

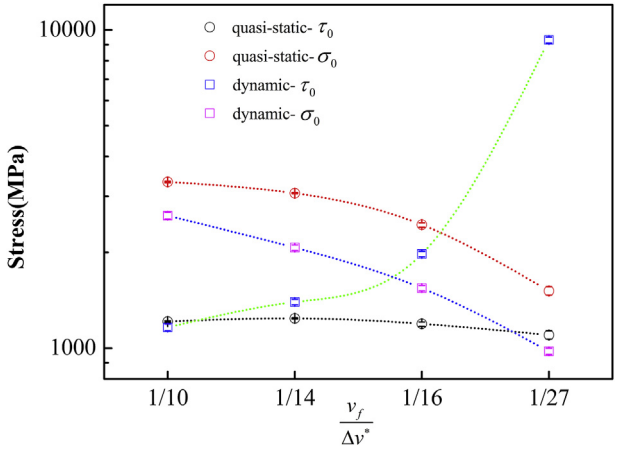

Fig. 5. Variation of the critical shear and normal stresses of the material with decreasing excess free volume under the two strain rates.

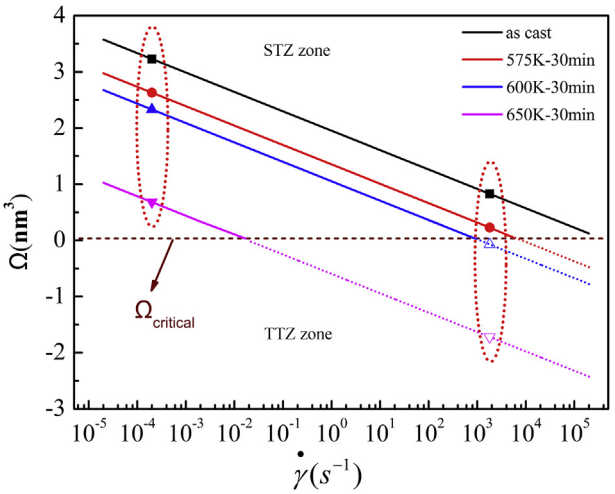

Fig. 6. The dependence of STZ volume on applied strain rate for all the samples. The points circled by dashed ellipses correspond to the strain rates adopted in this work.

to the dynamic level, the calculated Ω values of the samples "c" and "d" come to negative. As the STZ volume must be physically positive, the appearance of negative STZ volume means that Eq. (6) has reached its predictive limit and the calculated values are meaningless, which corresponds to the hollow points and the dashed lines in Fig. 6 (these meaningless points presented here are just to exhibit the trend of the variation). In other words, this implies the STZs cannot be activated. As a result, the TTZ-dominated brittle fracture will take place [32], instead of the ductile fracture dominated by STZ-mediated shear banding. This is in good agreement with the macroscopic fracture modes (Fig. 3(f) and (h)) and the microscopic fracture surface morphologies (Fig. 4(f) and (h)).

It is interesting to note that, with further increasing strain rate to 10^5 s^{-1} or higher level, the STZ volume of the samples "a" and "b" will also become negative (Fig. 6). This demonstrates that the samples with a relative high free volume concentration could also fracture in a normal tensile mode at room temperature, if the applied strain rate increase to a suitable level. It is reasonable to conclude that the DBT behavior of metallic glasses might be attributed to the competition between STZs and TTZs. The lower of the applied strain rate, the larger of the STZ volume will be, then the fracture of the metallic glasses will be dominated by STZ-mediated shear banding, finally showing a ductile fracture mode. On the contrary, the fracture will be dominated by TTZ-mediated-cavitation, resulting in a brittle tension mode. In general, STZ is aided by the free volume available in the material and initiates at the site where is abound of free volume. In the pioneering work of Wu and Spaepen [3], they suggested that a critical free volume is required for the amorphous alloy to exhibit good toughness. Therefore, it is reasonable to further speculate that a minimum available free volume is needed to aid to activate a STZ. If there is enough available (or mobile) free volume [55], STZ can be activated and ductile fracture will occur, otherwise, TTZ instead of STZ will be dominant to induce brittle fracture, i.e., DBT. In other words, no SZT activated means that the volume of STZ is extreme small or even equal to zero which is the DBT indicator in the present work. Many literatures [56–58] demonstrated that there would be larger free volume concentration at a higher strain rate. However, there is nearly no time for the movement and rearrangement of the atoms and associated free volume under a super-high strain rate, i.e., a higher strain rate will result in a less available free volume to assist in initiating STZ, indicating a TTZ dominant fracture will take place. Similarly, cryogenic temperature will also decrease the mobility of free volume and annealing will reduce the free volume concentration. Then, these three main factors (cryogenic temperature, annealing and high strain rate) will all reduce the available or mobile free volume. At a critical temperature, critical strain rate or critical free volume state due to annealing, there will be not enough available or mobile free volume to help to initiate STZ, then DBT will occur.

It must be addressed that there are many researchers dedicated to investigate the dependence of the applied strain rate on the mechanical properties of metallic glasses. However, the DBT behavior caused by the increasing of strain rate has been rarely reported so far. This derives in large part from that most of the works were carried out by compression test [58–63], which is very difficult to observe the transition of the fracture modes. Nevertheless, the results acquired from tensile tests also showed no DBT behavior [64,65]. According to the above analysis, the underlying reason for the absence of DBT behavior under tensile tests is that the applied strain rate is not high enough for the transition, which needs a suitable coordination of excess free volume and applied strain rate at a suitable temperature [21]. It is reasonable to predicate that with further increasing strain rate, samples with a relative large amount of excess free volume will suffer a DBT behavior.

5. Conclusion

In summary, quasi-static and dynamic tensile experiments were performed on the Vit105 metallic glass. A typical ductile-to-brittle transition was observed due to the increase of applied strain rates. Macroscopically, this transition can be well described by the Mohr-Coulomb criterion when the attention is paid to the ratio of the critical shear stress to the critical normal stress of the material under different strain rates. It is suggested that the increase of the applied strain rate will result in the decrease of the critical normal stress and the increase of the critical shear stress. Microscopically, the underlying mechanism of this transition can be revealed by the competition between the STZ-mediated shear banding and the TTZ-mediated cavitation. The present results are useful for understanding the deformation and fracture mechanism of metallic glasses and providing a method to guide the application of this type of disordered alloys.

Acknowledgements

The financial support from the National Natural Science Foundation of China (NSFC) under Grant Nos. 51171138, 51171137, 11372315, 11522221 and 51321003 are gratefully acknowledged.

References

[1] A.S. Argon, Mechanics and physics of brittle to ductile transitions in fracture, J. Eng. Mater. Technol. 123 (2001) 1–11.
[2] P. Gumbsch, J. Riedle, A. Hartmaier, H.F. Fischmeister, Controlling factors for the brittle-to-ductile transition in tungsten single crystals, Science 282 (1998) 1293–1295.
[3] T.W. Wu, F. Spaepen, The relation between embrittlement and structural relaxation of an amorphous metal, Philos. Mag. B 61 (1990) 739–750.
[4] G. Wang, Y.N. Han, X.H. Xu, F.J. Ke, B.S. Han, W.H. Wang, Ductile to brittle transition in dynamic fracture of brittle bulk metallic glass, J. Appl. Phys. 103 (2008) 093521–093525.
[5] R. Raghavan, P. Murali, U. Ramamurty, Ductile to brittle transition in the $Zr_{41.2}Ti_{13.75}Cu_{12.5}Ni_{10}Be_{22.5}$ bulk metallic glass, Intermetallics 14 (2006) 1051–1054.
[6] X.K. Xi, D.Q. Zhao, M.X. Pan, W.H. Wang, Y. Wu, J.J. Lewandowski, Fracture of brittle metallic glasses: brittleness or plasticity, Phys. Rev. Lett. 94 (2005) 125511–125514.
[7] Y. Wu, H.X. Li, Z.Y. Liu, G.L. Chen, Z.P. Lu, Interpreting size effects of bulk metallic glasses based on a size-independent critical energy density, Intermetallics 18 (2010) 157–160.
[8] Z.Q. Liu, W.H. Wang, M.Q. Jiang, Z.F. Zhang, Intrinsic factor controlling the deformation and ductile-to-brittle transition of metallic glasses, Philos. Mag. Lett. 94 (2014) 658–668.
[9] Y. Wu, H.X. Li, Z.B. Jiao, J.E. Gao, Z.P. Lu, Size effects on the compressive deformation behaviour of a brittle Fe-based bulk metallic glass, Philos. Mag. Lett. 90 (2010) 403–412.
[10] B. Gludovatz, S.E. Naleway, R.O. Ritchie, J.J. Kruzic, Size-dependent fracture toughness of bulk metallic glasses, Acta Mater. 70 (2014) 198–207.
[11] J.W. Cui, M. Calin, J. Eckert, Z.F. Zhang, Tensile fracture dynamics and intrinsic plasticity of metallic glasses, Appl. Phys. Lett. 102 (2013) 0319081–0319084.
[12] S.V. Madge, D.V. Louzguine-Luzgin, J.J. Lewandowski, A.L. Greer, Toughness, extrinsic effects and Poisson's ratio of bulk metallic glasses, Acta Mater. 60 (2012) 4800–4809.
[13] R. Narasimhan, P. Tandaiya, I. Singh, R.L. Narayan, U. Ramamurty, Fracture in metallic glasses: mechanics and mechanisms, Int. J. Fract. 191 (2015) 53–75.
[14] B.A. Sun, W.H. Wang, The fracture of bulk metallic glasses, Prog. Mater. Sci. 74 (2015) 211–307.
[15] X.J. Gu, S.J. Poon, G.J. Shiflet, J.J. Lewandowski, Compressive plasticity and toughness of a Ti-based bulk metallic glass, Acta Mater. 58 (2010) 1708–1720.
[16] R. Raghavan, V.V. Shastry, A. Kumar, T. Jayakumar, U. Ramamurty, Toughness of as-cast and partially crystallized composites of a bulk metallic glass, Intermetallics 17 (2009) 835–839.
[17] R. Raghavan, P. Murali, U. Ramamurty, On factors influencing the ductile-to-brittle transition in a bulk metallic glass, Acta Mater. 57 (2009) 3332–3340.
[18] F. Jiang, M.Q. Jiang, H.F. Wang, Y.L. Zhao, L. He, J. Sun, Shear transformation zone volume determining ductile–brittle transition of bulk metallic glasses, Acta Mater. 59 (2011) 2057–2068.
[19] G. Li, M.Q. Jiang, F. Jiang, L. He, J. Sun, Temperature-induced ductile-to-brittle transition of bulk metallic glasses, Appl. Phys. Lett. 102 (2013) 1719011–1719014.
[20] M.Q. Jiang, G. Wilde, J.H. Chen, C.B. Qu, S.Y. Fu, F. Jiang, L.H. Dai, Cryogenic-temperature-induced transition from shear to dilatational failure in metallic

glasses, Acta Mater. 77 (2014) 248–257.
[21] G. Li, M.Q. Jiang, F. Jiang, L. He, J. Sun, The ductile to brittle transition behavior in a Zr-based bulk metallic glass, Mater. Sci. Eng. A 625 (2015) 393–402.
[22] H.Q. Li, C. Fan, K.X. Tao, H. Choo, P.K. Liaw, Compressive behavior of a Zr-Based metallic glass at cryogenic temperatures, Adv. Mater. 18 (2006) 752–754.
[23] E.D. Tabachnikova, A.V. Podol'Skii, V.Z. Bengus, S.N. Smirnov, D.V. Luzgin, A. Inoue, Low-temperature plasticity anomaly in the bulk metallic glass $Zr_{64.13}Cu_{15.75}Ni_{10.12}Al_{10}$, Low. Temp. Phys. 34 (2008) 675–677.
[24] J.W. Qiao, H.L. Jia, Y. Zhang, P.K. Liaw, L.F. Li, Multi-step shear banding for bulk metallic glasses at ambient and cryogenic temperatures, Mater. Chem. Phys. 136 (2012) 75–79.
[25] Y.J. Huang, J. Shen, J.F. Sun, Z.F. Zhang, Enhanced strength and plasticity of a Ti-based metallic glass at cryogenic temperatures, Mater. Sci. Eng. A 498 (2008) 203–207.
[26] K.S. Yoon, M. Lee, E. Fleury, J.C. Lee, Cryogenic temperature plasticity of a bulk amorphous alloy, Acta Mater. 58 (2010) 5295–5304.
[27] J.W. Qiao, H.L. Jia, C.P. Chuang, E.W. Huang, G.Y. Wang, P.K. Liaw, Y. Ren, Y. Zhang, Low-temperature shear banding for a Cu-based bulk-metallic glass, Scr. Mater. 63 (2010) 871–874.
[28] A. Vinogradov, A. Lazarev, D.V. Louzguine-Luzgin, Y. Yokoyama, S. Li, A.R. Yavari, A. Inoue, Propagation of shear bands in metallic glasses and transition from serrated to non-serrated plastic flow at low temperatures, Acta Mater. 58 (2010) 6736–6743.
[29] F. Jiang, H.F. Wang, M.Q. Jiang, Y.L. Zhao, L. He, J. Sun, Ambient temperature embrittlement of a Zr-based bulk metallic glass, Mater. Sci. Eng. A 549 (2012) 14–19.
[30] R. Maaß, D. Klaumünzer, E. Preiß, P. Derlet, J. Löffler, Single shear-band plasticity in a bulk metallic glass at cryogenic temperatures, Scr. Mater. 66 (2012) 231–234.
[31] D. Pan, A. Inoue, T. Sakurai, M.W. Chen, Experimental characterization of shear transformation zones for plastic flow of bulk metallic glasses, Proc. Natl. Acad. Sci. U. S. A. 105 (2008) 14769–14772.
[32] M.Q. Jiang, Z. Ling, J.X. Meng, L.H. Dai, Energy dissipation in fracture of bulk metallic glasses via inherent competition between local softening and quasi-cleavage, Philos. Mag. 88 (2008) 407–426.
[33] A.S. Argon, M. Salama, The Second International Conference on rapidly quenched metals the mechanism of fracture in glassy materials capable of some inelastic deformation, Mater. Sci. Eng. 23 (1976) 219–230.
[34] X. Huang, Z. Ling, L.H. Dai, Ductile-to-brittle transition in spallation of metallic glasses, J. Appl. Phys. 116 (2014) 1435031–1435038.
[35] A. Slipenyuk, J. Eckert, Correlation between enthalpy change and free volume reduction during structural relaxation of $Zr_{55}Cu_{30}Al_{10}Ni_5$ metallic glass, Scr. Mater. 50 (2004) 39–44.
[36] Z. Evenson, R. Busch, Equilibrium viscosity, enthalpy recovery and free volume relaxation in a $Zr_{44}Ti_{11}Ni_{10}Cu_{10}Be_{25}$ bulk metallic glass, Acta Mater. 59 (2011) 4404–4415.
[37] Z.F. Zhang, J. Eckert, Unified tensile fracture criterion, Phys. Rev. Lett. 94 (2005) 0943011–0943014.
[38] Y. Chen, M.Q. Jiang, Y.J. Wei, L.H. Dai, Failure criterion for metallic glasses, Philos. Mag. 91 (2011) 4536–4554.
[39] R.T. Qu, J. Eckert, Z.F. Zhang, Tensile fracture criterion of metallic glass, J. Appl. Phys. 109 (2011) 08354401–08354412.
[40] Z.F. Zhang, G. He, J. Eckert, L. Schultz, Fracture mechanisms in bulk metallic glassy materials, Phys. Rev. Lett. 91 (2003) 0455051–0455054.
[41] R.T. Qu, M. Stoica, J. Eckert, Z.F. Zhang, Tensile fracture morphologies of bulk metallic glass, J. Appl. Phys. 108 (2010) 0635091–0635099.
[42] Z.Q. Liu, R.T. Qu, Z.F. Zhang, Elasticity dominates strength and failure in metallic glasses, J. Appl. Phys. 117 (2015) 01490101–01490111.
[43] A.S. Argon, Plastic deformation in metallic glasses, Acta Metall. 27 (1979) 47–58.
[44] J.J. Lewandowski, A.L. Greer, Temperature rise at shear bands in metallic glasses, Nat. Mater. 5 (2005) 15–18.
[45] R.L. Narayan, P. Tandaiya, R. Narasimhan, U. Ramamurty, Wallner lines, crack velocity and mechanisms of crack nucleation and growth in a brittle bulk metallic glass, Acta Mater. 80 (2014) 407–420.
[46] A. Christiansen, J.B. Shortall, The fracture toughness and fracture morphology of polyester resins, J. Mater. Sci. 11 (1976) 1113–1124.
[47] J.J. Lewandowski, A.K. Thurston, P. Lowhaphandu, Fracture toughness of amorphous metals and composites, in: MRS Proceedings, Cambridge Univ Press, 2002, pp. CC9.3.1–CC9.3.7.
[48] J.J. Lewandowski*, W.H. Wang, A.L. Greer, Intrinsic plasticity or brittleness of metallic glasses, Philos. Mag. Lett. 85 (2005) 77–87.
[49] Z.F. Zhang, E. Jürgen, L. Schultz, Difference in compressive and tensile fracture mechanisms of $Zr_{59}Cu_{20}Al_{10}Ni_8Ti_3$ bulk metallic glass, Acta Mater. 51 (2003) 1167–1179.
[50] A.C. Lund, C.A. Schuh, Yield surface of a simulated metallic glass, Acta Mater. 51 (2003) 5399–5411.
[51] C.A. Schuh, A.C. Lund, Atomistic basis for the plastic yield criterion of metallic glass, Nat. Mater. 2 (2003) 449–452.
[52] J. Caris, J.J. Lewandowski, Pressure effects on metallic glasses, Acta Mater. 58 (2010) 1026–1036.
[53] W.L. Johnson, K. Samwer, A universal criterion for plastic yielding of metallic glasses with a $(T/T_g)^{(2/3)}$ temperature dependence, Phys. Rev. Lett. 95 (2005) 195501–195504.
[54] M.D. Demetriou, J.S. Harmon, M. Tao, D. Gang, K. Samwer, W.L. Johnson, Cooperative shear model for the rheology of glass-forming metallic liquids, Phys. Rev. Lett. 97 (2006) 0655021–0655024.
[55] M.Q. Jiang, G. Wilde, F. Jiang, L.H. Dai, Understanding ductile-to-brittle transition of metallic glasses from shear transformation zone dilatation, Theor. Appl. Mech. Lett. 5 (2015) 200–204.
[56] P. De Hey, J. Sietsma, A. Van Den Beukel, Structural disordering in amorphous $Pd_{40}Ni_{40}P_{20}$ induced by high temperature deformation, Acta Mater. 46 (1998) 5873–5882.
[57] L.F. Liu, L.H. Dai, Y.L. Bai, B.C. Wei, Initiation and propagation of shear bands in Zr-based bulk metallic glass under quasi-static and dynamic shear loadings, J. Non-Cryst. Solids 351 (2005) 3259–3270.
[58] W. Zheng, Y.J. Huang, J. Shen, Influence of strain-rate on compressive-deformation behavior of a Zr–Cu–Ni–Al bulk metallic glass at cryogenic temperature, Mater. Sci. Eng. A 528 (2011) 6855–6859.
[59] T. Mukai, T.G. Nieh, Y. Kawamura, A. Inoue, K. Higashi, Effect of strain rate on compressive behavior of a $Pd_{40}Ni_{40}P_{20}$ bulk metallic glass, Intermetallics 10 (2002) 1071–1077.
[60] S. González, G.Q. Xie, D.V. Louzguine-Luzgin, J.H. Perepezko, A. Inoue, Deformation and strain rate sensitivity of a Zr–Cu–Fe–Al metallic glass, Mater. Sci. Eng. A 528 (2011) 3506–3512.
[61] T.H. Chen, C.K. Tsai, The microstructural evolution and mechanical properties of zr-based metallic glass under different strain rate compressions, Materials 8 (2015) 1831–1840.
[62] W. Zheng, Y.J. Huang, G.Y. Wang, P.K. Liaw, J. Shen, Influence of strain rate on compressive deformation behavior of a Zr-Cu-Ni-Al bulk metallic glass at room temperature, Metall. Mater. Trans. A 42 (2011) 1491–1498.
[63] Y.F. Xue, H.N. Cai, L. Wang, F.C. Wang, H.F. Zhang, Effect of loading rate on failure in Zr-based bulk metallic glass, Mater. Sci. Eng. A 473 (2008) 105–110.
[64] T. Mukai, T.G. Nieh, Y. Kawamura, A. Inoue, K. Higashi, Dynamic response of a $Pd_{40}Ni_{40}P_{20}$ bulk metallic glass in tension, Scr. Mater. 46 (2002) 43–47.
[65] A.V. Sergueeva, N.A. Mara, J.D. Kuntz, D.J. Branagan, A.K. Mukherjee, Shear band formation and ductility of metallic glasses, Mater. Sci. Eng. A 383 (2004) 219–223.